

NONLOCAL MICROPLANE CONCRETE MODEL WITH RATE EFFECT AND LOAD CYCLES. I: GENERAL FORMULATION

By Toshiaki Hasegawa¹ and Zdeněk P. Bažant,² Fellow, ASCE

ABSTRACT: The nonlocal microplane model for concrete is improved to describe unloading, reloading, cyclic loading, and the rate effect. The differences compared to the previous formulation are: (1) Normal strain component on the microplane is not split into its volumetric and deviatoric parts—rather the normal component is made dependent on the lateral normal strains on the microplane; and (2) instead of considering on each microplane only one shear strain vector parallel to the shear stress vector, the shear strain is represented by two independent components on the microplane. To introduce rate effect, the stress-strain law for each microplane component is described by a generalized Maxwell model—a series coupling of a linear viscous element and an elastoplastic-fracturing element. Nonlinear unloading-reloading hysteresis rules with back- and objective-stresses are developed to introduce hysteresis. The model is then combined with nonlocal theory to enable describing localization phenomena and avoid spurious mesh sensitivity due to strain softening. The numerical implementation in finite-element programs is described. The study consists of two parts: part I deals with the general formulation (part II deals with experimental verification).

INTRODUCTION

The heterogeneity of concretes and brittleness of its matrix are responsible for complex nonlinear triaxial behavior with strain-softening damage. To describe such behavior, many types of models for concrete have been developed and investigated. They may be grouped into two basic categories—the macroscopic phenomenologic models and the micromechanics-based models. The hypoelastic models, plasticity models, endochronic models, fracturing theory, and continuum damage mechanics models belong to the former category. The constitutive models in the second category are more limited at present. The microplane model is one effective model based on certain simplified micromechanics ideas. It has been proven to describe many experimentally observed features of concretes as well as rocks and soils (Bažant 1984; Bažant and Oh 1985; Bažant and Prat 1988; Bažant and Ožbolt 1990; Ožbolt and Bažant 1991; Carol et al. 1992). The microplane model has been combined with the nonlocal theory in order to make it applicable to localized fracture behavior and size effects, and to avoid spurious mesh sensitivity in finite element analysis (Bažant and Ožbolt 1990; Ožbolt and Bažant 1991).

The present study (Hasegawa and Bažant 1991) attempts to improve and generalize the previously developed microplane model in several respects, particularly with regard to response to cyclic loading as influenced by the loading rate. This influence is manifested in the shape and width of the

¹Struct. Res. Engr., Shimizu Corp., 3-4-17 Etchujima, Koto-ku, Tokyo 135, Japan.

²Walter P. Murphy Prof. of Civ. Engrg., Northwestern Univ., 2145 Sheridan Rd., Evanston, IL 60208-3109.

Note. Discussion open until January 1, 1994. Separate discussions should be submitted for the individual papers in this symposium. To extend the closing date one month, a written request must be filed with the ASCE Manager of Journals. The manuscript for this paper was submitted for review and possible publication on September 23, 1991. This paper is part of the *Journal of Materials in Civil Engineering*, Vol. 5, No. 3, August, 1993. ©ASCE, ISSN 0899-1561/93/0003-0372/\$1.00 + \$.15 per page. Paper No. 2741.

hysteresis loops. The loading rate of course also strongly affects the response to monotonic loading.

It should be mentioned that another partly similar but in some basic aspects different model, with different advantages, was developed at Northwestern University (Ožbolt and Bažant 1991) at the same time as the model presented here. Because of scope limitations, a comparison of these two versions of the cyclic microplane model with rate effect is relegated to a subsequent study.

MODIFICATION AND SIMPLIFICATION OF PREVIOUS MICROPLANE MODEL

A detailed description of the concept of microplane model and its evolution, beginning with the idea of Taylor (1938), was given in Bažant and Prat (1988) and is not repeated here. The following hypotheses, in some respects different from those used in the previous work, were adopted for the development of the present generalized cyclic and rate-dependent version of the model. (The Latin lower-case subscripts refer to Cartesian coordinates x_i , $i = 1, 2, 3$.)

Hypothesis I

The strains on any microplane are the resolved components of the macroscopic strain tensor ϵ_{ij} (this represents a tensorial kinematic constraint).

Hypothesis II

The microplane resists not only normal strains ϵ_N , but also in-plane shear-strain vectors (ϵ_{TK} , ϵ_{TM}), whose direction within each microplane is the same as that of the shear stress vector (σ_{TK} , σ_{TM}).

Hypothesis III

The normal-stress increments on a microplane depend on the resolved lateral strains ϵ_L on the same microplane.

Hypothesis IV

The inelastic shear-stress vector increment on each microplane depends on the resolved normal component of the macroscopic stress tensor σ_{ij} on the same microplane (this represents an additional static constraint).

Hypothesis V

Constitutive laws for the normal and shear components on the microplanes (microconstitutive law) are based on a generalized Maxwell rheologic model in which a linear viscous element is coupled in series with an elastoplastic-fracturing element.

Hypothesis VI

The microconstitutive laws for the normal and shear components on each microplane are mutually independent.

Hypothesis VI was justified in Bažant and Prat (1988). The decoupling of volumetric, deviatoric, and shear responses on the microplane seems at first an oversimplification. But success in the modeling of test data indicates that the appropriate coupling of the volumetric and deviatoric responses on the macroscopic level is obtained through the coupling of microplanes of all orientations due to the kinematic constraint. In contrast to the previous

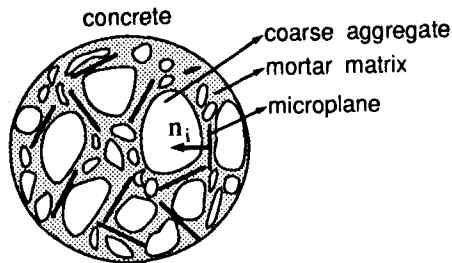
formulations by Bažant and Prat (1988) and Carol et al. (1991), the normal microplane components are not split into volumetric and deviatoric parts in the present model.

According to hypothesis I, the normal-strain component and the strain vector components on a microplane of direction cosines n_i are

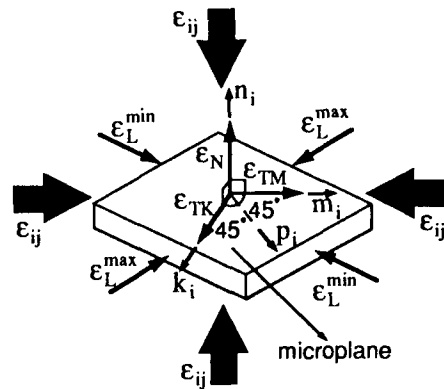
$$\epsilon_N = n_j \epsilon_j'' = n_j n_k \epsilon_{jk} \dots \dots \dots (1a)$$

$$\epsilon_{Ni} = n_i n_j n_k \epsilon_{jk} \dots \dots \dots (1b)$$

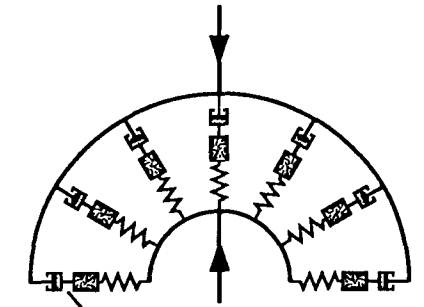
In the previous microplane model, the shear-strain response was defined, for the sake of simplicity, only in terms of magnitudes $\epsilon_T = \sqrt{\epsilon_{Ti} \epsilon_{Ti}} = [n_k \epsilon_{jm} n_m (\epsilon_{jk} - n_j n_i \epsilon_{ik})]^{1/2}$. With this definition, the strain magnitudes are always positive. But this makes it impossible to describe the cyclic response on microplanes. To avoid this limitation, two in-plane unit coordinate vectors \mathbf{k} and \mathbf{m} , normal to each other, are introduced on each microplane as shown in Fig. 1(b), and two shear components ϵ_{TK} , ϵ_{TM} in those directions



(a)

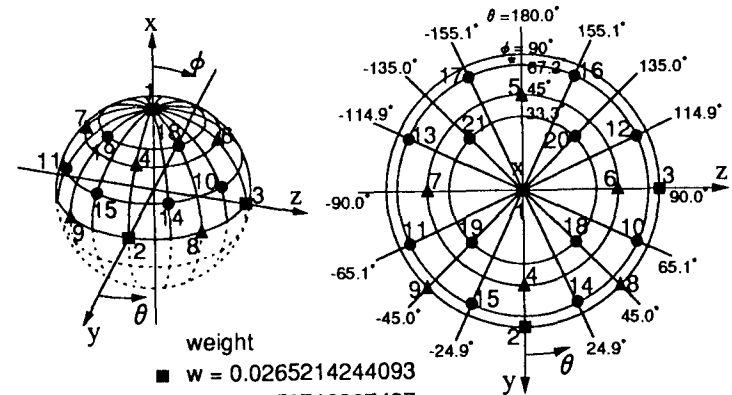


(b)



generalized Maxwell model for each microplane
linear viscous element elasto-plastic-fracturing element

(c)



weight
 ■ $w = 0.0265214244093$
 ● $w = 0.0250712367487$
 ▲ $w = 0.0199301476312$

(d)

FIG. 1. (Continued)

FIG. 1. (a) Microplanes in Concrete; (b) Unit Vectors \mathbf{n} , \mathbf{k} , \mathbf{m} ; and \mathbf{p} on Microplane; (c) Microplane System (without Shear Response) and Generalized Maxwell Model for Each Microplane; (d) Numerical Integration Points on Unit Hemisphere for 21 Integration Points Formula

are considered. Since the directions of the vector \mathbf{k} and \mathbf{m} must be fixed at the beginning of calculations, some kind of rule to determine these directions is necessary. The rule must not have a significant bias for any direction; i.e., the frequency of various directions within the microplanes taken by vectors \mathbf{m} and \mathbf{n} must be about the same. This is approximately achieved by the following simple rule: vector \mathbf{m} of microplane 1 is determined to be

normal to the z-axis, vector \mathbf{m} of microplane 2 normal to the x-axis, vector \mathbf{m} of microplane 3 normal to the y-axis, vector \mathbf{m} of microplane 4 normal again to the z-axis, and so on. Then for vector \mathbf{m} normal to z-axis

$$m_1 = \frac{n_2}{\sqrt{n_1^2 + n_2^2}}; \quad m_2 = \frac{-n_1}{\sqrt{n_1^2 + n_2^2}}; \quad m_3 = 0 \quad \dots \dots \dots (2a)$$

but $m_1 = 1; m_2 = 0; m_3 = 0$ if $n_1 = n_2 = 0$.

For vector \mathbf{m} normal to x-axis

$$m_2 = \frac{n_3}{\sqrt{n_2^2 + n_3^2}}; \quad m_3 = \frac{-n_2}{\sqrt{n_2^2 + n_3^2}}; \quad m_1 = 0 \quad \dots \dots \dots (2b)$$

but $m_1 = 0; m_2 = 1; m_3 = 0$ if $n_2 = n_3 = 0$.

For vector \mathbf{m} normal to y axis

$$m_1 = \frac{-n_3}{\sqrt{n_1^2 + n_3^2}}; \quad m_3 = \frac{n_1}{\sqrt{n_1^2 + n_3^2}}; \quad m_2 = 0 \quad \dots \dots \dots (2b)$$

but $m_1 = 0; m_2 = 0; m_3 = 1$ if $n_1 = n_3 = 0$.

After determining vector \mathbf{m} , vector \mathbf{k} is calculated for each microplane as $\mathbf{k} = \mathbf{m} \times \mathbf{n}$. According to hypothesis II, the in-plane shear strain components in the \mathbf{k} and \mathbf{m} directions on a microplane of direction cosines n_i are

$$\varepsilon_{TK} = k_j \varepsilon_j^n = k_j n_i \varepsilon_{ij} = \frac{1}{2} (k_i n_j + k_j n_i) \varepsilon_{ij} \quad \dots \dots \dots (3a)$$

$$\varepsilon_{TM} = m_j \varepsilon_j^n = m_j n_i \varepsilon_{ij} = \frac{1}{2} (m_i n_j + m_j n_i) \varepsilon_{ij} \quad \dots \dots \dots (3b)$$

where symmetry of ε_{ij} was exploited to symmetrize these expressions. The separate treatment of ε_{TK} and ε_{TM} brings about an improvement over the previous microplane formulation by Bažant and Prat (1988), but it increases the number of variables.

INCREMENTAL MACROSCOPIC STRESS-STRAIN RELATIONSHIP

The incremental microconstitutive relations are written separately for the normal component and the shear components in the K and M directions

$$d\sigma_N = C_N d\varepsilon_N - d\sigma_N'' \quad \text{for normal component} \quad \dots \dots \dots (4a)$$

$$d\sigma_{TK} = C_{TK} d\varepsilon_{TK} - d\sigma_{TK}'' \quad \text{for } K\text{-shear component} \quad \dots \dots \dots (4b)$$

$$d\sigma_{TM} = C_{TM} d\varepsilon_{TM} - d\sigma_{TM}'' \quad \text{for } M\text{-shear component} \quad \dots \dots \dots (4c)$$

in which $d\sigma_N, d\sigma_{TK},$ and $d\sigma_{TM}$ = incremental microstresses; $C_N, C_{TK},$ and C_{TM} = incremental elastic stiffnesses; and $d\sigma_N'', d\sigma_{TK}'',$ and $d\sigma_{TM}''$ = inelastic microstress increments. Note that there is no coupling between K -shear and M -shear (decoupling hypothesis for shear).

Using the principle of virtual work (i.e., equality of virtual works of the macrostresses and microstresses), we can write

$$\frac{4\pi}{3} d\sigma_{ij} \delta\varepsilon_{ij} = 2 \int_S (d\sigma_N \delta\varepsilon_N + d\sigma_{TK} \delta\varepsilon_{TK} + d\sigma_{TM} \delta\varepsilon_{TM}) f(\mathbf{n}) dS \quad \dots \dots (5)$$

in which $\delta\varepsilon_{ij}, \delta\varepsilon_N, \delta\varepsilon_{TK},$ and $\delta\varepsilon_{TM}$ = small variations of the macroscopic strain tensor and of the microstrain components on a microplane. The constant $4\pi/3$ means that the macroscopic work is taken over the volume of a unit sphere. The factor 2 on the right-hand side arises because the microscopic work needs to be integrated only over the surface of a unit hemisphere S . The function $f(\mathbf{n})$ is a weight function for the normal directions \mathbf{n} , which in general can introduce anisotropy of the material in its initial state. We will use $f(\mathbf{n}) = 1$, which means isotropy. Expressing $\delta\varepsilon_N, \delta\varepsilon_{TK},$ and $\delta\varepsilon_{TM}$ from (1) and (3) and substituting them into (5), we can get

$$\frac{4\pi}{3} d\sigma_{ij} \delta\varepsilon_{ij} = 2 \int_S \left[n_i n_j d\sigma_N + \frac{d\sigma_{TK}}{2} (k_i n_j + k_j n_i) + \frac{d\sigma_{TM}}{2} (m_i n_j + m_j n_i) \right] f(\mathbf{n}) dS \delta\varepsilon_{ij} \quad \dots \dots \dots (6)$$

This variational equation must hold for any variations $\delta\varepsilon_{ij}$; therefore we can delete $\delta\varepsilon_{ij}$; and substituting (4) we obtain

$$d\sigma_{ij} = \frac{3}{2\pi} \int_S \left[n_i n_j d\sigma_N + \frac{d\sigma_{TK}}{2} (k_i n_j + k_j n_i) + \frac{d\sigma_{TM}}{2} (m_i n_j + m_j n_i) \right] f(\mathbf{n}) dS \quad \dots \dots \dots (7a)$$

$$d\sigma_{ij} = \frac{3}{2\pi} \int_S \left[n_i n_j (C_N d\varepsilon_N - d\sigma_N'') + \frac{1}{2} (k_i n_j + k_j n_i) (C_{TK} d\varepsilon_{TK} - d\sigma_{TK}'') + \frac{1}{2} (m_i n_j + m_j n_i) (C_{TM} d\varepsilon_{TM} - d\sigma_{TM}'') \right] f(\mathbf{n}) dS \quad \dots \dots \dots (7b)$$

Eqs. (1) and (3) may now be here substituted for $\varepsilon_N, \varepsilon_{TK},$ and ε_{TM} . This finally yields the macroscopic incremental stress-strain relation

$$d\sigma_{ij} = C_{ijrs} d\varepsilon_{rs} - d\sigma_{ij}'' \quad \dots \dots \dots (8)$$

in which C_{ijrs} denotes the incremental elastic stiffness tensor

$$C_{ijrs} = \frac{3}{2\pi} \int_S \left[n_i n_j n_r n_s C_N + \frac{1}{4} (k_i n_j + k_j n_i) (k_r n_s + k_s n_r) C_{TK} + \frac{1}{4} (m_i n_j + m_j n_i) (m_r n_s + m_s n_r) C_{TM} \right] f(\mathbf{n}) dS \quad \dots \dots \dots (9)$$

and $d\sigma_{ij}''$ denotes the inelastic stress increments

$$d\sigma_{ij}'' = \frac{3}{2\pi} \int_S \left[n_i n_j d\sigma_N'' + \frac{1}{2} (k_i n_j + k_j n_i) d\sigma_{TK}'' + \frac{1}{2} (m_i n_j + m_j n_i) d\sigma_{TM}'' \right] f(\mathbf{n}) dS \quad \dots \dots \dots (10)$$

For the initial isotropic elastic response we can substitute the initial moduli C_N^0 and C_T^0 for C_N and C_{TK}, C_{TM} in (9), and set $f(\mathbf{n}) = 1$. Since these moduli are independent of the microplane direction, we could integrate (9) explicitly

if the unit vectors \mathbf{k} and \mathbf{m} were also known explicitly. However, they are not explicit, being calculated numerically as described before.

For initial elasticity we can substitute the initial moduli C_N^0 and C_T^0 for C_N and C_{TK} , C_{TM} in (4), and set $d\sigma_N'' = d\sigma_{TK}'' = d\sigma_{TM}'' = 0$. Then we have $d\sigma_{TK} = C_T^0 d\varepsilon_{TK}$ and $d\sigma_{TM} = C_T^0 d\varepsilon_{TM}$ for shears. From that, $|d\sigma_T| = C_T^0 |d\varepsilon_T|$, where $|d\sigma_T| = \sqrt{d\sigma_{TK}^2 + d\sigma_{TM}^2}$ and $|d\varepsilon_T| = \sqrt{d\varepsilon_{TK}^2 + d\varepsilon_{TM}^2}$. This is the same relation as that used in the previous microplane model involving normal and shear components (Bažant 1984) (in which the shear vectors were characterized by three components in the Cartesian coordinates x_i ; $i = 1, 2, 3$). Therefore the expressions derived in that study apply

$$C_N^0 = \frac{E}{(1 - 2\nu)} \quad \dots \quad (11a)$$

$$C_T^0 = \frac{(1 - 4\nu)E}{(1 - 2\nu)(1 + \nu)} \quad \dots \quad (11b)$$

in which E and ν = Young's modulus and Poisson's ratio.

One can now realize from (11) that only Poisson's ratios ν within the range $-1 \leq \nu \leq 0.25$ can be obtained with the present microplane model, while the microplane model with separate volumetric, deviatoric, and shear components (Bažant and Prat 1988) can describe elastic behavior with any thermodynamically possible Poisson's ratio $-1 \leq \nu \leq 0.5$. However, the disadvantage of the limited range of Poisson's ratio in the present model does not seem very serious for concrete, since for usual concretes $0.15 \leq \nu \leq 0.22$. In general, of course, we do not advocate abandoning the previous formulation with the full range of ν , which is in principle more realistic. The present restriction on the range of ν is due to avoiding a split of normal microplane components into volumetric and deviatoric ones, which brings about a simplification of the formulation.

RHEOLOGIC MODEL FOR RATE EFFECT IN MICROCONSTITUTIVE LAW

For cyclic behavior it is important to specify appropriate rate-dependent microconstitutive models. In this study a series coupling of a linear viscous element and an elastoplastic-fracturing element is adopted for the microconstitutive law on each microplane [Fig. 1(c)]. For the sake of brevity of notation, let ε and σ now represent any of the microstrains ε_N , ε_{TK} , and ε_{TM} and microstresses σ_N , σ_{TK} , and σ_{TM} . The model is described by the differential equation

$$\frac{d\sigma}{dt} = C' \frac{d\varepsilon}{dt} - \frac{\sigma}{\rho} \quad \dots \quad (12)$$

where $C' = C^v$ for virgin loading; $C' = C^{ur}$ for unloading and reloading; t = time; ρ = relaxation time of the viscous element; and C' = current tangential stiffness of the elastoplastic-fracturing element, which takes the value of either C^v or C^{ur} depending on the loading-unloading-reloading criteria described later. When (12) is solved by using a central difference approximation, numerical difficulties or instabilities may be encountered in the case of strain softening, and even if the solution is numerically stable, a large error is usually accumulated and the stress is not reduced exactly to zero at very large strains.

To avoid these difficulties, the exponential algorithm, initially developed for aging creep of concrete (Bažant 1971, 1988), is applied in this study in a similar way as in an alternative nonlocal microplane model of Bažant and Ožbolt (1990). To achieve unrestricted numerical stability, we need to re-write (12) so that it involves a positive incremental stiffness or unload-reload stiffness throughout the entire range of hardening and softening

$$\frac{d\sigma}{dt} = C^{ur} \frac{d\varepsilon}{dt} - \frac{\sigma}{\beta} \quad \dots \quad (13)$$

$$\frac{1}{\beta} = \frac{1}{\rho} + (C^{ur} - C')\sigma \frac{d\varepsilon}{dt} \quad \dots \quad (14)$$

in which β = a quasi-relaxation time for the purpose of calculation. When we apply (13) and (14) to finite steps, it is most accurate to take the values of C^{ur} , C' , ρ , and σ for the middle of the time step (t_r, t_{r+1}) , denoted with subscript $r + 1/2$, in which r = number of the step ($r = 1, 2, \dots$)

$$\frac{d\sigma}{dt} = C_{r+1/2}^{ur} \frac{d\varepsilon}{dt} - \frac{\sigma}{\beta_{r+1/2}} \quad \dots \quad (15)$$

$$\frac{1}{\beta_{r+1/2}} = \frac{1}{\rho_{r+1/2}} + (C_{r+1/2}^{ur} - C'_{r+1/2})\sigma_{r+1/2} \frac{\Delta\varepsilon}{\Delta t} \quad \dots \quad (16)$$

$C_{r+1/2}^{ur}$ and $\beta_{r+1/2}$ in these equations are assumed to be constant for the duration of each time step; however, to calculate $\sigma_{r+1/2}$, $C_{r+1/2}^{ur}$, and $C'_{r+1/2}$, we need σ_{r+1} , C_{r+1}^{ur} , and C'_{r+1} , which means that numerical iterations of the time step are necessary. The general solution of (15) is then exactly

$$\sigma(t) = A e^{-(t-t_r)/\beta_{r+1/2}} + C_{r+1/2}^{ur} \beta_{r+1/2} \frac{d\varepsilon}{dt} \quad \dots \quad (17)$$

in which A = an integration constant. From the initial condition $\sigma = \sigma_r$ at $t = t_r$, the integration constant can be calculated as $A = \sigma_r - C_{r+1/2}^{ur} \beta_{r+1/2} d\varepsilon/dt$, and then

$$\sigma(t) = \sigma_r e^{-(t-t_r)/\beta_{r+1/2}} + [1 - e^{-(t-t_r)/\beta_{r+1/2}}] C_{r+1/2}^{ur} \beta_{r+1/2} \frac{d\varepsilon}{dt} \quad \dots \quad (18)$$

For the end of the time step, $t = t_{r+1} = t_r + \Delta t$, we have

$$\sigma_r + \Delta\sigma = \sigma_r e^{-\Delta z} + \frac{1}{\Delta z} (1 - e^{-\Delta z}) C_{r+1/2}^{ur} \Delta\varepsilon \quad \dots \quad (19)$$

where $\Delta z = \Delta t/\beta_{r+1/2}$. We can rewrite (19) in the form of (4)

$$\Delta\sigma = \frac{1}{\Delta z} (1 - e^{-\Delta z}) C_{r+1/2}^{ur} \Delta\varepsilon - (1 - e^{-\Delta z}) \sigma_r = C \Delta\varepsilon - \Delta\sigma'' \quad \dots \quad (20)$$

where

$$C = \frac{1}{\Delta z} (1 - e^{-\Delta z}) C_{r+1/2}^{ur} \quad \dots \quad (21)$$

$$\Delta\sigma'' = (1 - e^{-\Delta z}) \sigma_r \quad \dots \quad (22)$$

MICROCONSTITUTIVE LAW FOR NORMAL COMPONENTS

To be able to model the response to hydrostatic pressure, we must assume the stress-strain curve for the normal component to be the same as for the volumetric component of the previous microplane model. But then reasonable postpeak strain-softening would not be obtained for uniaxial or biaxial compression. This problem is circumvented by hypothesis III. The purpose of including a dependence on lateral strains is to achieve the following: (1) The normal strain response would not be the same as the volumetric or hydrostatic response except when the lateral strains are the same as the normal strain, which is the case of hydrostatic loading; while at the same time (2) the normal response would be more brittle when the difference between the normal and lateral strains is large, i.e., it would exhibit more strain softening.

To implement hypothesis III, we need to derive equations for the maximum and minimum principal values ϵ_L^{\max} , ϵ_L^{\min} of lateral strain on each microplane. To this end we introduce another in-plane unit vector \mathbf{p} , whose angle with the unit vectors \mathbf{k} and \mathbf{m} is 45° , as shown in Fig. 1(b); $\mathbf{p} = (\mathbf{k} + \mathbf{m})/\sqrt{2}$. The lateral normal strains in the directions of \mathbf{k} , \mathbf{m} , and \mathbf{p} are

$$\epsilon_K = k_i k_j \epsilon_{ij} \dots\dots\dots (23a)$$

$$\epsilon_M = m_i m_j \epsilon_{ij} \dots\dots\dots (23b)$$

$$\epsilon_P = p_i p_j \epsilon_{ij} \dots\dots\dots (23c)$$

Considering Mohr's circle for in-plane strains in the microplane, we can get the maximum and minimum principal values ϵ_L^{\max} , ϵ_L^{\min} of the lateral strain on each microplane

$$\epsilon_L^{\max} = \frac{\epsilon_K + \epsilon_M}{2} + \sqrt{\left(\frac{\epsilon_K - \epsilon_M}{2}\right)^2 + \left(\frac{\epsilon_K + \epsilon_M}{2} - \epsilon_P\right)^2} \dots\dots\dots (24)$$

$$\epsilon_L^{\min} = \frac{\epsilon_K + \epsilon_M}{2} - \sqrt{\left(\frac{\epsilon_K - \epsilon_M}{2}\right)^2 + \left(\frac{\epsilon_K + \epsilon_M}{2} - \epsilon_P\right)^2} \dots\dots\dots (25)$$

which are invariant. It is useful to define a lateral-deviatoric strain ϵ_{LD} that combines ϵ_L^{\max} and ϵ_L^{\min} into one strain invariant for the microplane

$$\epsilon_{LD} = |\epsilon_N - \epsilon_L^{\max}| + |\epsilon_N - \epsilon_L^{\min}| \dots\dots\dots (26)$$

To be able to change the normal response from the hydrostatic stress-strain response, which always has a positive slope, to plastic response (zero slope) and softening response (negative slope), the following hardening-softening function $\phi(\epsilon_{LD})$ in terms of ϵ_{LD} may be introduced [Fig. 2(b)]:

$$\phi(\epsilon_{LD}) = \frac{1}{1 + \left(\frac{\epsilon_{LD}}{\epsilon_{LD}^1}\right)^m} \dots\dots\dots (27a)$$

$$\phi(\epsilon_{LD}) = \phi^p \quad \text{when } \epsilon_{LD} = \epsilon_{LD}^p \dots\dots\dots (27b)$$

$$\phi(\epsilon_{LD}) = 0 \quad \text{when } \epsilon_L^{\max} > 0 \dots\dots\dots (27c)$$

in which $\epsilon_{LD}^1 = \epsilon_{LD}$ value when $\phi(\epsilon_{LD}) = 0.5$; $m =$ a constant that specifies

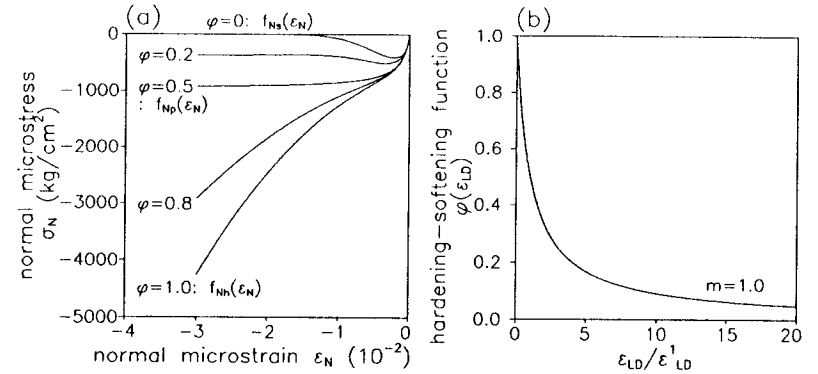


FIG. 2. (a) Dependence of Normal Compression Microstress-Strain Curve on Lateral Strain; (b) Hardening-Softening Function for Normal Compression

the shape of the curve $\phi(\epsilon_{LD})$; and $\phi^p =$ value corresponding to the case of plastic response.

Now we try to set weight functions in terms of $\phi(\epsilon_{LD})$ and use them to obtain a gradual transition from hydrostatic response to plastic response and softening response for the virgin loading curve of the normal-strain component of the microplane; for $0 \leq \epsilon_{LD} \leq \epsilon_{LD}^p$

$$\sigma_N(\epsilon_N, \epsilon_{LD}) = \left(\frac{\phi(\epsilon_{LD}) - \phi^p}{1 - \phi^p}\right) f_{Nh}(\epsilon_N) + \left(\frac{1 - \phi(\epsilon_{LD})}{1 - \phi^p}\right) f_{Np}(\epsilon_N) \dots (28a)$$

For $\epsilon_{LD}^p < \epsilon_{LD}$

$$\sigma_N(\epsilon_N, \epsilon_{LD}) = \left(\frac{\phi(\epsilon_{LD})}{\phi^p}\right) f_{Np}(\epsilon_N) + \left(\frac{\phi^p - \phi(\epsilon_{LD})}{\phi^p}\right) f_{Ns}(\epsilon_N) \dots\dots (28b)$$

in which $f_{Nh}(\epsilon_N) =$ hydrostatic loading curve of normal component when $\epsilon_{LD} = 0$; $f_{Np}(\epsilon_N) =$ plastic loading curve of normal component when $\epsilon_{LD} = \epsilon_{LD}^p$; and $f_{Ns}(\epsilon_N) =$ softening loading curve of normal component when $\epsilon_{LD} = \infty$ [Fig. 2(a)].

To obtain the loading tangential stiffness, we need to differentiate (28); for $0 \leq \epsilon_{LD} \leq \epsilon_{LD}^p$

$$\frac{d\sigma_N(\epsilon_N, \epsilon_{LD})}{d\epsilon_N} = \left(\frac{\phi(\epsilon_{LD}) - \phi^p}{1 - \phi^p}\right) \frac{df_{Nh}(\epsilon_N)}{d\epsilon_N} + \left(\frac{1 - \phi(\epsilon_{LD})}{1 - \phi^p}\right) \frac{df_{Np}(\epsilon_N)}{d\epsilon_N} \dots\dots\dots (29a)$$

For $\epsilon_{LD}^p < \epsilon_{LD}$

$$\frac{d\sigma_N(\epsilon_N, \epsilon_{LD})}{d\epsilon_N} = \left(\frac{\phi(\epsilon_{LD})}{\phi^p}\right) \frac{df_{Np}(\epsilon_N)}{d\epsilon_N} + \left(\frac{\phi^p - \phi(\epsilon_{LD})}{\phi^p}\right) \frac{df_{Ns}(\epsilon_N)}{d\epsilon_N} \dots (29b)$$

Similarly, the transition for the linear unload-reload stiffnesses C_N^{ur0} ($\sigma_N^u, \epsilon_N^u, \epsilon_{LD}$) may be written as follows; for $0 \leq \epsilon_{LD} \leq \epsilon_{LD}^p$

$$C_N^{ur0}(\sigma_N^u, \epsilon_N^u, \epsilon_{LD}) = \left(\frac{\phi(\epsilon_{LD}) - \phi^p}{1 - \phi^p}\right) C_{Nh}^{ur0}(\sigma_N^u, \epsilon_N^u)$$

$$+ \left(\frac{1 - \phi(\epsilon_{LD})}{1 - \phi^p} \right) C_{Np}^{ur0}(\sigma_N^u, \epsilon_N^u) \dots \dots \dots (30a)$$

For $\epsilon_{LD}^p < \epsilon_{LD}$

$$C_{Np}^{ur0}(\sigma_N^u, \epsilon_N^u, \epsilon_{LD}) = \left(\frac{\phi(\epsilon_{LD})}{\phi^p} \right) C_{Np}^{ur0}(\sigma_N^u, \epsilon_N^u) + \left(\frac{\phi^p - \phi(\epsilon_{LD})}{\phi^p} \right) C_{Ns}^{ur0}(\sigma_N^u, \epsilon_N^u) \dots \dots \dots (30b)$$

in which $C_{Nh}^{ur0}(\sigma_N^u, \epsilon_N^u)$ = hydrostatic linear unload-reload stiffness of the normal component when $\epsilon_{LD} = 0$; $C_{Np}^{ur0}(\sigma_N^u, \epsilon_N^u)$ = plastic linear unload-reload stiffness of the normal component when $\epsilon_{LD} = \epsilon_{LD}^p$; $C_{Ns}^{ur0}(\sigma_N^u, \epsilon_N^u)$ = softening linear unload-reload stiffness of the normal component when $\epsilon_{LD} = \infty$; σ_N^u and ϵ_N^u = stress and strain at the start of unloading.

In the previous microplane model, virgin loading curves for strain-softening on each microplane were formulated using a single exponential function, $\sigma = C^0 e^{-1/\epsilon^a} \epsilon^p$. With this kind of equation, however, one cannot adjust the peak stress, peak strain, and postpeak ductility individually. It is more versatile to introduce equations that can do so. Therefore, in this study the following virgin loading curves are used for pre- and postpeak tensile regions of the normal component [Fig. 3(a)].

For $0 \leq \epsilon_N \leq \epsilon_{NT}^0$ (prepeak)

$$\sigma_N = \sigma_{NT}^0 \left[1 - \left(1 - \frac{\epsilon_N}{\epsilon_{NT}^0} \right)^{C_N^0 \epsilon_{NT}^0 / \sigma_{NT}^0} \right] \quad \text{with } \epsilon_{NT}^0 = \frac{\sigma_{NT}^0}{\zeta_{NT} C_N^0} \dots \dots (31a)$$

For $\epsilon_{NT}^0 < \epsilon_N$ (postpeak)

$$\sigma_N = \sigma_{NT}^0 \exp \left[- \left(\frac{\epsilon_N - \epsilon_{NT}^0}{\epsilon_{NT}^0} \right)^{p_{NT}} \right] \quad \text{with } \epsilon_{NT}^0 = \gamma_{NT} \epsilon_{NT}^0 = \frac{\gamma_{NT} \sigma_{NT}^0}{\zeta_{NT} C_N^0} \dots \dots \dots (31b)$$

In (31), σ_{NT}^0 = peak stress of the curve; ζ_{NT} = a parameter that controls the peak strain ϵ_{NT}^0 ; and γ_{NT} = a parameter that controls ϵ_{NT}^0 . At the strain $\epsilon_N = \epsilon_{NT}^0 + \epsilon_{NT}^0$, the stress decreases to σ_{NT}^0/e in the softening region; p_{NT} = a parameter that changes the shape of the softening curve. Thus we can control the shape of the stress-strain curve with these four parameters quite easily, which is important for being able to adjust properly the macroscopic response with the microplane model; C_N^0 = initial modulus for the normal component, which can be determined from (11).

For the compression range of the normal component, we must specify the equations for softening, plastic, and hydrostatic stress-strain curves, as mentioned before. The same types of equation as for tension are assumed as for compression softening of the normal component [Fig. 3(a)].

For $0 \geq \epsilon_N \geq \epsilon_{NC}^0$ (prepeak)

$$f_{Ns}(\epsilon_N) = \sigma_N = \sigma_{NC}^0 \left[1 - \left(1 - \frac{\epsilon_N}{\epsilon_{NC}^0} \right)^{C_N^0 \epsilon_{NC}^0 / \sigma_{NC}^0} \right] \quad \text{with } \epsilon_{NC}^0 = \frac{\sigma_{NC}^0}{\zeta_{NC} C_N^0} \dots \dots \dots (32a)$$

for $\epsilon_{NC}^0 > \epsilon_N$ (postpeak)

$$f_{Ns}(\epsilon_N) = \sigma_N = \sigma_{NC}^0 \exp \left[- \left(\frac{\epsilon_N - \epsilon_{NC}^0}{\epsilon_{NC}^0} \right)^{p_{NC}} \right] \quad \text{with } \epsilon_{NC}^0 = \gamma_{NC} \epsilon_{NC}^0 = \frac{\gamma_{NC} \sigma_{NC}^0}{\zeta_{NC} C_N^0} \dots \dots \dots (32b)$$

For the hydrostatic curve of the normal component, we introduce the relation

$$f_{Nh}(\epsilon_N) = \sigma_N = \left[\frac{C_N^0}{\left(\frac{\epsilon_N}{\epsilon_a} \right)^{p_H} + 1} + \frac{C_N^f}{\left(\frac{\epsilon_N}{\epsilon_b} \right)^{-q_H} + 1} \right] \epsilon_N \dots \dots \dots (33)$$

in which C_N^f = asymptotic final modulus for normal compression as shown in Fig. 3(b); ϵ_a and ϵ_b = strain values that characterize the shape of the curve; and p_H (≤ 1) and q_H (> -1) = exponents that also change the shape. With this equation, we have six parameters to be fixed. Eq. (33) can control the final tangent stiffness of the hydrostatic curve; the equation of the previous model with five parameters cannot.

For the plastic curve of the normal component, the first part of the hydrostatic curve with $p_H = 1$ is adopted, for the sake of simplicity

$$f_{Np}(\epsilon_N) = \sigma_N = \frac{C_N^0}{\left(\frac{\epsilon_N}{\epsilon_a} \right) + 1} \epsilon_N \dots \dots \dots (34)$$

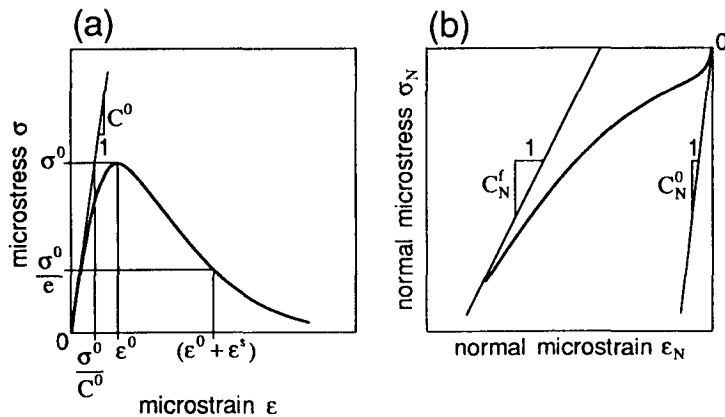


FIG. 3. (a) Strain-Softening Curve for Microplane; (b) Hydrostatic Curve for Normal Compression

For unloading and reloading, the initial moduli of the normal component, C_N^0 , are used as the linear unload-reload stiffnesses C_{Nt}^{ur0} and C_{Nc}^{ur0} for the case of hydrostatic and plastic responses and also in the prepeak region of the tensile or compressive softening response. On the other hand, for the case of tensile or compressive softening after the peak stress, the following damage evolution is considered for linear unload-reload stiffness C_{Ns}^{ur0} .

For $0 \leq \varepsilon_N \leq \varepsilon_{NT}^0$ (prepeak tension) and $0 \geq \varepsilon_N \geq \varepsilon_{NC}^0$ (prepeak compression)

$$C_{Ns}^{ur0} = C_N^0 \dots \dots \dots (35a)$$

For $\varepsilon_N > \varepsilon_{NT}^0$ (postpeak tension)

$$C_{Ns}^{ur0} = \alpha_{NT} C_N^0 + (1 - \alpha_{NT}) \frac{\sigma_{NT}^{u0}}{\varepsilon_{NT}^{u0} - \xi_{NT}} \quad \text{with } \xi_{NT} = \varepsilon_{NT}^0 - \frac{\sigma_{NT}^0}{C_N^0} \dots \dots \dots (35b)$$

For $\varepsilon_N < \varepsilon_{NC}^0$ (postpeak compression)

$$C_{Ns}^{ur0} = \alpha_{NC} C_N^0 + (1 - \alpha_{NC}) \frac{\sigma_{NC}^{u0}}{\sigma_{NC}^{u0} - \xi_{NC}} \quad \text{with } \xi_{NC} = \varepsilon_{NC}^0 - \frac{\sigma_{NC}^0}{C_N^0} \dots \dots \dots (35c)$$

in which α_{NT} , α_{NC} = weight constants, which describe the proportions of progressive damage in tension and compression softening; σ_{NT}^{u0} and σ_{NC}^{u0} = stresses at the start of unloading for tension and compression softening; ε_{NT}^{u0} and ε_{NC}^{u0} = strains at the start of unloading for tension and compression softening; ξ_{NT} and ξ_{NC} = plastic residual strains after complete unloading from the peak stress to zero stress. Thus, with parameter C_{Ns}^{ur0} we can control the elastoplastic-fracturing behavior for the case of softening in normal microplane component.

MICROCONSTITUTIVE LAW FOR SHEAR COMPONENTS

We know that shear behavior usually depends on the compressive stress normal to the shear plane. We will take this dependence into account in the constitutive law for the shear component on the microplane according to hypothesis IV. In the previous microplane model, this effect was modeled through the confining stress $\sigma_c = \sigma_{ii}/3$, which had the advantage that σ_{ii} is the same for all the microplanes. However, a frictional effect such as this would be better considered individually on each microplane since the shear response on each microplane is independent and the magnitudes of normal stress on various microplanes are different. Therefore, in this study it is assumed that the peak shear stress value on each microplane depends on the resolved normal component of the macroscopic stress tensor σ_{ij} on the same microplane individually. The resolved normal component S_N of the macroscopic stress tensor σ_{ij} on a microplane whose direction cosines are n_i is

$$S_N = n_j \sigma_j^i = n_j n_k \sigma_{jk} \dots \dots \dots (36)$$

The virgin loading curve of *K*-shear component and *M*-shear component must be specified as identical since they differ only in the chosen directions within the microplane. We use for shear the same form of strain-softening equation as for the normal component [Fig. 3(a)].

For $0 \leq |\varepsilon_T| \leq |\varepsilon_T^0|$ (prepeak)

$$\sigma_T = \tau^0 \left[1 - \left(1 - \frac{\varepsilon_T}{\varepsilon_T^0} \right)^{C_T^0 \varepsilon_T^0 / \tau^0} \right] \quad \text{with } \varepsilon_T^0 = \frac{\tau^0}{\zeta_T C_T^0} \dots \dots \dots (37a)$$

For $|\varepsilon_T^0| < |\varepsilon_T|$ (postpeak)

$$\sigma_T = \tau^0 \exp \left[- \left(\frac{\varepsilon_T - \varepsilon_T^0}{\sigma_T^0} \right)^{p_T} \right] \quad \text{with } \varepsilon_T^0 = \gamma_T \varepsilon_T^0 = \frac{\gamma_T \tau^0}{\zeta_T C_T^0} \dots \dots \dots (37b)$$

in which subscript *T* refers to *K*-shear (*TK*) or *M*-shear (*TM*); τ^0 = peak stress, which depends on S_N ; ζ_T = a parameter that controls the peak strain ε_T^0 ; and γ_T = a parameter that controls ε_T^0 . At the strain $\varepsilon_T = \varepsilon_T^0 + \varepsilon_T^s$, the stress decreases to τ^0/e in the strain-softening region; p_T = a parameter controlling the shape of the softening curve. Unlike the normal component, (37) is applied for both tension and compression. The only difference between tension and compression is the sign of the peak stress τ^0 ; i.e., $\tau^0 > 0$ in tension and $\tau^0 < 0$ in compression.

The concept of shear frictional coefficient μ is utilized to model the dependence of shear peak stress τ^0 on S_N .

For tension of shear

$$\tau^0 = +\sigma_T^0 - \mu S_N \quad \text{when } S_N < 0 \dots \dots \dots (38a)$$

$$\tau^0 = +\sigma_T^0 \quad \text{when } S_N \geq 0 \dots \dots \dots (38b)$$

For compression of shear

$$\tau^0 = -\sigma_T^0 + \mu S_N \quad \text{when } S_N < 0 \dots \dots \dots (38c)$$

$$\tau^0 = -\sigma_T^0 \quad \text{when } S_N \geq 0 \dots \dots \dots (38d)$$

in which σ_T^0 = peak shear stress at zero normal stress. Thus, our stress-strain curve for shear has five parameters, σ_T^0 , ζ_T , γ_T , p_T , and μ .

For straight-line unloading and reloading, the initial modulus of the shear component, C_T^0 , is used as the linear unload-reload stiffness C_T^{ur0} in the case of the prepeak region. On the other hand, after the peak stress, the following damage evolution is considered for the linear unload-reload stiffness C_T^{ur0} for straight-line response.

For $0 \leq |\varepsilon_T| \leq |\varepsilon_T^0|$ (prepeak)

$$C_T^{ur0} = C_T^0 \dots \dots \dots (39a)$$

For $|\varepsilon_T| > |\varepsilon_T^0|$ (postpeak)

$$C_T^{ur0} = \alpha_T C_T^0 + (1 - \alpha_T) \frac{\sigma_T^u}{\varepsilon_T^u - \xi_T} \quad \text{with } \xi_T = \varepsilon_T^0 - \frac{\tau^0}{C_T^0} \dots \dots \dots (39b)$$

in which α_T = a weight constant that describes progressive damage for shear softening; σ_T^u , ε_T^u = stress and strain at the start of unloading; and ξ_T = plastic residual strain after complete unloading from the peak stress to zero stress. Thus, C_T^{ur0} models the elastoplastic-fracturing microconstitutive law for the softening in shear.

LOADING, UNLOADING AND RELOADING IN MICROCONSTITUTIVE RELATIONS

Macroscopic stress-strain relations for cyclic loading require proper loading-unloading-reloading criteria for each microplane component. Since our

microplane model is based on a kinematic constraint and the response on each microplane can be described only (or mainly) by microstrain components, it seems preferable to express the loading criteria in terms of microstrains only. Let each microstrain $\epsilon_N, \epsilon_{TK}, \epsilon_{TM}$ and microstress component $\sigma_N, \sigma_{TK}, \sigma_{TM}$ be defined as ϵ and σ , for the sake of simplicity. The following loading-unloading-reloading criteria are used for all the components.

Loading

$$\text{when } \sigma_r > 0, \quad \Delta\epsilon_{r+1} > 0, \quad \epsilon_{r+1} \geq \epsilon_{\max} \quad \dots \quad (40a)$$

$$\text{when } \sigma_r < 0, \quad \Delta\epsilon_{r+1} < 0, \quad \epsilon_{r+1} \leq \epsilon_{\min} \quad \dots \quad (40b)$$

Unloading

$$\text{when } \sigma_r > 0, \quad \Delta\epsilon_{r+1} < 0, \quad \epsilon_{r+1} < \epsilon_{\max} \quad \dots \quad (40c)$$

$$\text{when } \sigma_r < 0, \quad \Delta\epsilon_{r+1} > 0, \quad \epsilon_{r+1} > \epsilon_{\min} \quad \dots \quad (40d)$$

Reloading

$$\text{when } \sigma_r > 0, \quad \Delta\epsilon_{r+1} > 0, \quad \epsilon_{r+1} < \epsilon_{\max} \quad \dots \quad (40e)$$

$$\text{when } \sigma_r < 0, \quad \Delta\epsilon_{r+1} < 0, \quad \epsilon_{r+1} > \epsilon_{\min} \quad \dots \quad (40f)$$

in which σ_r = microstress of each component at the end of the previous load step; ϵ_{r+1} = microstrain of each component at the present load step; $\Delta\epsilon_{r+1} = \epsilon_{r+1} - \epsilon_r$ = incremental microstrain of each component; and ϵ_{\max} and ϵ_{\min} = maximum and minimum microstrains in the history.

The loading-unloading-reloading criteria in (40) with linear unload-reload stiffnesses C_N^{ur0} [(30) and (35)] and C_T^{ur0} [(39)] can be used in order to describe the cyclic behavior of each component. However, numerical simulations with C_N^{ur0} and C_T^{ur0} revealed that the hysteresis loops are too narrow. Wider hysteresis loops on the microplane are necessary to obtain proper hysteresis on the macrolevel. The reason is that hysteresis loops govern energy dissipation and the basic hypothesis of the microplane model is energy equivalence between the macro- and microlevels. Nonlinear unloading-reloading hysteresis rules with back-stress and objective-stress are developed for this purpose. The hysteresis rules are applied to the case of unloading or reloading in the strain-softening regions. The microplane back-stress σ_b is defined as

$$\sigma_{b,r+1} = \sigma_r \quad \text{when } \Delta\epsilon_r \Delta\epsilon_{r+1} < 0 \quad \dots \quad (41a)$$

$$\sigma_{b,r+1} = \sigma_{b,r} \quad \text{when } \Delta\epsilon_r \Delta\epsilon_{r+1} \geq 0 \quad \dots \quad (41b)$$

in which subscripts r and $r + 1$ refer to the previous and current numerical steps. The microplane objective-stress σ_{ob} is defined as

$$\sigma_{ob} = 0 \quad \text{when unloading} \quad \dots \quad (42a)$$

$$\sigma_{ob} = \sigma^u \quad \text{when reloading} \quad \dots \quad (42b)$$

in which σ^u = stress at the start of unloading from the virgin loading curve; σ_b and σ_{ob} are set when the microplane is unloading or reloading. We introduce the following unloading-reloading function $F^{ur}(\sigma)$ in terms of microstress σ on the unloading or reloading branch:

$$F^{ur}(\sigma) = \left| \frac{\sigma_b - \sigma}{\sigma_{ob} - \sigma_b} \right| \quad \dots \quad (43)$$

This function is nondimensional and its values vary from 0 to 1. The unloading tangent stiffness $C^u(\sigma)$ and the reloading tangent stiffness $C^r(\sigma)$ are (see Fig. 4)

$$C^u(\sigma) = [(U_{\min} - U_{\max})F^{ur}(\sigma) + U_{\max}]C^{ur0} \quad \dots \quad (44a)$$

$$C^r(\sigma) = [(R_{\min} - R_{\max})F^{ur}(\sigma) + R_{\max}]C^{ur0} \quad \dots \quad (44b)$$

in which U_{\min} and U_{\max} = nondimensional ratios determining the minimum and maximum unloading tangent stiffnesses C_{\min}^u and C_{\max}^u (i.e., $C_{\min}^u = U_{\min}C^{ur0}$ and $C_{\max}^u = U_{\max}C^{ur0}$); R_{\min} and R_{\max} = nondimensional ratios determining the minimum and maximum reloading tangent stiffnesses C_{\min}^r and C_{\max}^r (i.e., $C_{\min}^r = R_{\min}C^{ur0}$ and $C_{\max}^r = R_{\max}C^{ur0}$). Using the foregoing hysteresis rules, one can get hysteresis loops such as that depicted in Fig. 4(a).

CYCLIC LOADING RULES FOR MICROCONSTITUTIVE RELATIONS

The foregoing rules apply separately to the tension and compression regions of each microplane component. The borderline between the tension and compression regions is given by zero microplane stress. To establish a complete cyclic loading model for the microplane, the foregoing rule must be extended to the entire range of tensile and compressive microplane

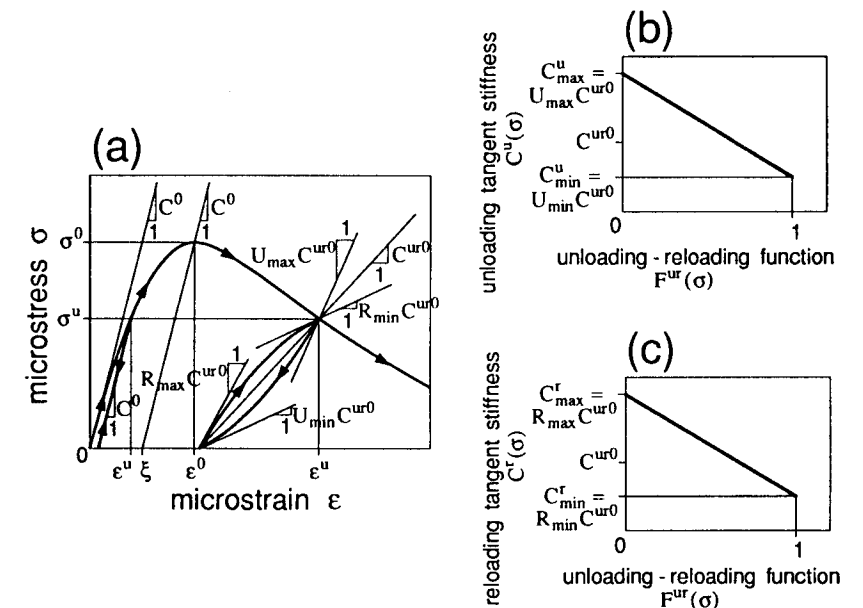


FIG. 4. (a) Unloadings and Reloadings from and to Points on Virgin Microstress-Strain Curve; (b) Unloading Tangent Stiffness $C^u(\sigma)$; (c) Reloading Tangent Stiffness $C^r(\sigma)$

stresses. The basic idea to do this is as follows: (1) The virgin stress-strain curves for both tension and compression are unique regardless of the number of cycles or the strain history; (2) the transition between the tension and compression regions involves horizontal plateaus; and (3) the virgin stress-strain curves can be horizontally shifted along the strain axes to the starting point of unloading or reloading. Many possible cases of the cyclic rule based on this basic idea were tried numerically and compared to the uniaxial compressive and tensile tests from the literature.

The cyclic rule for the normal component which was determined in this way is illustrated by the idealized (partially exaggerated) stress-strain curves in Fig. 5(a) (softening curve $f_N(\epsilon_N)$ is used for compression). With the cyclic rule for the normal component, the origin of the compression stress-strain curve is fixed; however, the origin of the tension curve is shifted as shown. In the example of Fig. 5(a), the first cycle enters tensile softening, and then reverts to compression. Before going into compressive stress, there is a plateau, which corresponds to closing of microcracks. The compression region begins always at the origin (zero strain); however, the origin of tension is shifted every time when unloading from the compression region crosses the strain axis.

The cyclic rule for the shear component is shown by the idealized stress-strain curves in Fig. 5(b). The origins of the stress-strain curves for both tension and compression regions are fixed. In the example shown, the strain cycles are similar to those used in the previous example of normal component; however, the stress responses are very different. After the unloading curves reach the strain axis, there are always plateaus of zero stress. This assumption is needed to model experimental observations showing that for large deformations almost no stress change occurs in crack shear (aggregate interlock) tests with stress reversals. Such behavior is due to free play between asperities or between the faces of opened cracks, which need to come into contact before the stress can reverse its sign.

NONLOCAL MICROPLANE MODEL

The microplane model described so far deals only with the point properties of the macroscopic continuum approximating the average response of the heterogeneous material, under macroscopically uniform strain. This is in-

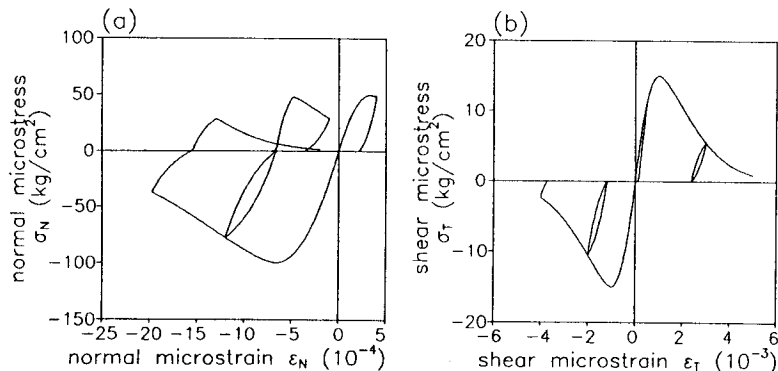


FIG. 5. (a) Cyclic Rule for Normal Component; (b) Cyclic Rule for Shear Component

sufficient for describing the localization phenomena and size effects. To this end, as is by now well established, one must introduce some type of a nonlocal concept.

In the original (imbricate) nonlocal theory (Bažant et al. 1984) the total strain was assumed to be nonlocal. But this has the disadvantage that the differential equilibrium equations and the boundary conditions are not the same as those of the local continuum theory. More recently (Pijaudier-Cabot and Bažant 1987; Bažant and Pijaudier-Cabot 1988; Bažant and Lin 1988) it has been shown that the nonlocal aspects of strain-softening can be captured while preserving the same forms of the equilibrium equations and the boundary conditions as those of the local continuum theory. In the new nonlocal damage theory, only the variables associated with strain softening are nonlocal while all the other variables, particularly the elastic strain, are local. This new nonlocal concept, which was combined with the microplane model for time-independent monotonic response of concrete in Bažant and Ožbolt (1990), is adopted in this study.

To render the microplane model nonlocal, we replace the local values of microplane stiffnesses C_N, C_{TK}, C_{TM} [(9)] and inelastic microstresses $d\sigma_N^i, d\sigma_{TK}^i, d\sigma_{TM}^i$ [(10)] with the nonlocal values $\bar{C}_N, \bar{C}_{TK},$ and \bar{C}_{TM} and $d\bar{\sigma}_N^i, d\bar{\sigma}_{TK}^i, d\bar{\sigma}_{TM}^i$ (the overbars mean "nonlocal"). These nonlocal values are calculated on the basis of the nonlocal microstrains $\bar{\epsilon}_N, \bar{\epsilon}_{TK}, \bar{\epsilon}_{TM}$, which represent the resolved components of the nonlocal macroscopic strain tensor $\bar{\epsilon}_{ij}$. Thus, one always needs both local and nonlocal variables and must calculate both responses for each component on each microplane. When a microplane is loading (hardening or softening), we use the nonlocal values in (9) and (10), and when a microplane is unloading or reloading, we use the local values. The nonlocal macroscopic strain tensor $\bar{\epsilon}_{ij}$ is calculated as

$$\bar{\epsilon}_{ij}(\mathbf{x}) = \frac{1}{V_r(\mathbf{x})} \int_V \alpha(\mathbf{s} - \mathbf{x}) \epsilon_{ij}(\mathbf{s}) dV = \int_V \alpha'(\mathbf{x}, \mathbf{s}) \epsilon_{ij}(\mathbf{s}) dV \dots \dots \dots (45)$$

in which

$$V_r(\mathbf{x}) = \int_V \alpha(\mathbf{s} - \mathbf{x}) dV \dots \dots \dots (46a)$$

$$\alpha'(\mathbf{x}, \mathbf{s}) = \frac{\alpha(\mathbf{s} - \mathbf{x})}{V_r(\mathbf{x})} \dots \dots \dots (46b)$$

\mathbf{x} and \mathbf{s} = coordinate vectors; $\alpha(\mathbf{x})$ = weight function, which is treated as a material property; V = volume of the entire structure; $V_r(\mathbf{x})$ has approximately but not exactly the same meaning as the representative volume in the statistical theory of heterogeneous materials.

Initially the weight function $\alpha(\mathbf{x})$ was assumed as the normal (Gaussian) distribution function. Recently Bažant proposed to use a computationally more efficient quartic bell-shaped function, which vanishes for distances greater than $r_1 = kl$ (Fig. 6)

$$\text{for } \lambda \leq 1: \alpha(\mathbf{x}) = (1 - \lambda^2)^2; \quad \text{for } \lambda > 1: \alpha(\mathbf{x}) = 0 \dots \dots \dots (47)$$

in which $\lambda = r/r_1 = r/kl$ and for the one-dimensional case

$$r = |x_1|; \quad k = \frac{15}{16} \dots \dots \dots (48a)$$

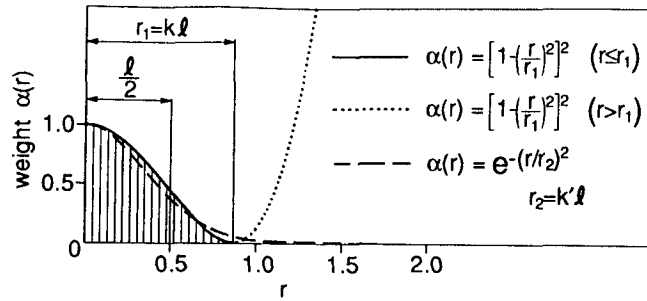


FIG. 6. Weight Functions for Nonlocal Averaging

For two-dimensional case

$$r = \sqrt{x_1^2 + x_2^2}; \quad k = \frac{\sqrt{3}}{2} \quad \dots \dots \dots (48b)$$

For three-dimensional case

$$r = \sqrt{x_1^2 + x_2^2 + x_3^2}; \quad k = \left(\frac{35}{64}\right)^{1/3} \quad \dots \dots \dots (48c)$$

where x_i = Cartesian coordinates; k = constants determined from the condition that the volume under the function $\alpha(\mathbf{x})$ should be equal to the volume under a function $\bar{\alpha}(\mathbf{x})$ that is uniform, $\bar{\alpha}(\mathbf{x}) = 1$ for $r \leq l/2$, and $\bar{\alpha}(\mathbf{x}) = 0$ for $r > l/2$. Here l is the characteristic length of nonlocal continuum (which gives the size of the representative volume).

NUMERICAL ALGORITHM IN FINITE-ELEMENT ANALYSIS

The present nonlocal microplane model has been introduced in a usual nonlinear finite-element program using initial stiffness method. One reason why the initial stiffness method is used is the nonsymmetry of the structural stiffness matrix, which is caused by treating only the inelasticity as nonlocal. Another reason is numerical convergence in the softening regime of the structure. Although the initial stiffness method sometimes gives slow convergence, it always converges and leads to stable iterations when the stress and strain increments due to iterations are accumulated.

In the first iteration of the first load step, the total elastic structural stiffness matrix \mathbf{K} is assembled using the specified Young's modulus and Poisson's ratio of the material. In each load step, the following numerical algorithm is employed.

1. At the beginning of each iteration, \mathbf{K} is used to estimate a trial structural incremental displacement vector $\Delta \mathbf{u}$ by solving the equation $\Delta \mathbf{u} = \mathbf{K}^{-1} \Delta \mathbf{f}$, where $\Delta \mathbf{f}$ is the nodal force increment due to prescribed force and displacement at the present load step or the residual nodal force from the previous iteration. Then one calculates the incremental local macroscopic strains $\Delta \epsilon_{ij}$ for all the integration points of all finite elements, and also the incremental nonlocal macroscopic strains $\Delta \bar{\epsilon}_{ij}$ from (45) and (46).

2. The incremental local microstrains $\Delta \epsilon_{N}$, $\Delta \epsilon_{TK}$, and $\Delta \epsilon_{TM}$ are calculated

for each microplane at each integration point of each finite element using (1) and (3) with $\Delta \epsilon_{ij}$. The incremental nonlocal microstrains $\Delta \bar{\epsilon}_{N}$, $\Delta \bar{\epsilon}_{TK}$, and $\Delta \bar{\epsilon}_{TM}$ are also evaluated from $\Delta \bar{\epsilon}_{ij}$. Then, for normal, K -shear, and M -shear components of both local and nonlocal strains on each microplane, loading, unloading, or reloading is judged using (40). Depending on the loading-unloading-reloading condition, the local and nonlocal values of the microstiffnesses C_N , C_{TK} , C_{TM} , \bar{C}_N , \bar{C}_{TK} , and \bar{C}_{TM} and the local and nonlocal inelastic microstresses $d\sigma''_N$, $d\sigma''_{TK}$, $d\sigma''_{TM}$, $d\bar{\sigma}''_N$, $d\bar{\sigma}''_{TK}$, and $d\bar{\sigma}''_{TM}$ are calculated based on the aforementioned microconstitutive models. If there is hardening or softening (virgin loading) on a microplane we use the nonlocal microstiffnesses and inelastic microstresses; on the other hand, if unloading or reloading occurs on a microplane, the local values are used to calculate macroscopic incremental stiffness C_{ij} , [(9)] and macroscopic inelastic stress increment $d\sigma''_{ij}$ [(10)] for the integration point of the finite element. Then the macroscopic total stress increment $d\sigma_{ij}$ [(18)] and the macroscopic total stress σ_{ij} are calculated.

3. Based on the calculated total stresses at each integration point in each finite element, the total equivalent nodal forces \mathbf{f}^{LQ} are evaluated and assembled for the whole structure. The residual nodal forces \mathbf{f}^R are calculated as $\mathbf{f}^R = \mathbf{f} - \mathbf{f}^{LQ}$, in which \mathbf{f} is the total nodal force due to the prescribed force and displacement at the present load step, or the residual nodal force of the previous iteration.

4. The norm ratio ω of the residual nodal forces, defined as $\omega = [\Sigma (\mathbf{f}^R)^2 / \Sigma (\mathbf{f}^L)^2]^{1/2}$, is calculated to judge convergence of the iterations. In this study, if $\omega \leq 0.01$, the iteration process is judged to have converged, and the calculation advances to the next load step. If $\omega > 0.01$, one returns to step 1 and starts the next iteration.

To implement the step-by-step calculation, a number of characteristic microstrain and microstress values for each microplane need to be stored in the computer memory. Their number is 43 (= 15 + 2 x 14) per microplane (Table 1). Since in this study the Bažant and Oh's (1986) integration

TABLE 1. Characteristic Values for State of Each Microplane to Be Stored in Memory

Value		Normal		Shear K and M	
(1)	(2)	Tension (3)	Compression (4)	Tension (5)	Compression (6)
Strain in previous iteration	ϵ_r	○	○	○	○
Maximum strain	ϵ_{max}	○	—	○	—
Minimum strain	ϵ_{min}	—	○	—	○
Strain at back-stress	ϵ_b	○	○	○	○
Strain at zero stress after complete unloading	ϵ_p	○	○	○	○
Strain at origin of curve	ϵ_z	○	—	—	—
Stress in previous iteration	σ_r	○	○	○	○
Stress at start of unloading	σ''	○	○	○	○
Back-stress	σ_b	○	○	○	○
Linear unload-reload stiffness	C^{ur0}	○	○	○	○

Note: ○ means necessary to be stored in memory.

formula with 21 points on a hemisphere is used [Fig. 1(d)], and since we have both local and nonlocal components, we need to store $1,806 (= 2 \times 21 \times 43)$ values for each integration point of each finite element.

CONCLUSION

The present improved and extended formulation of the microplane model for concrete bears considerable promise with regard to numerical finite-element analysis of concrete structures. [Application to the analysis of test data is done in part II (Hasegawa and Bažant 1993); in which detailed conclusions are to be found.]

ACKNOWLEDGMENT

The present results have been obtained under a joint research program between Shimizu Corporation, Tokyo, and Northwestern University. The first author wishes to thank Shimizu Corporation for giving him the opportunity to conduct this research at Northwestern University.

APPENDIX. REFERENCES

- Bažant, Z. P. (1971). "Numerically stable algorithm with increasing time steps for integral-type aging creep." *Proc., 1st Int. Conf. on Struct. Mech. in Reactor Technol.*, T. A. Jaeger, ed., West Berlin, Germany, 4, Part H, 119–126.
- Bažant, Z. P. (1984). "Microplane model for strain-controlled inelastic behavior." *Mechanics of engineering materials*, C. S. Desai and R. H. Gallagher, eds., John Wiley and Sons, New York, N.Y., 45–59.
- Bažant, Z. P. (1988). "Improvements of microplane model." *Int. Res. Notes*, Northwestern University, Evanston, Ill.
- Bažant, Z. P., Belytschko, T. B., and Chang, T.-P. (1984). "Continuum theory for strain-softening." *J. Engrg. Mech.*, ASCE, 110(12), 1666–1692.
- Bažant, Z. P., and Chern, J.-C. (1985). "Strain softening with creep and exponential algorithm." *J. Engrg. Mech.*, ASCE, 111(3), 391–415.
- Bažant, Z. P., and Lin, F.-B. (1988). "Nonlocal smeared cracking model for concrete fracture." *J. Struct. Engrg.*, ASCE, 114(11), 2493–2510.
- Bažant, Z. P., and Oh, B. H. (1985). "Microplane model for progressive fracture of concrete and rock." *J. Engrg. Mech.*, ASCE, 111(4), 559–582.
- Bažant, Z. P., and Oh, B. H. (1986). "Efficient numerical integration on the surface of a sphere." *Zeitschrift für Angewandte Mathematik und Mechanik*, Leipzig, Germany, 66(1), 37–49.
- Bažant, Z. P., and Ožbolt, J. (1990). "Nonlocal microplane model for fracture, damage, and size effect in structures." *J. Engrg. Mech.*, ASCE, 116(11), 2485–2505.
- Bažant, Z. P., and Pijaudier-Cabot, G. (1988). "Nonlocal continuum damage, localization instability and convergence." *J. Appl. Mech.*, 55(2), 287–293.
- Bažant, Z. P., and Prat, P. C. (1988a). "Microplane model for brittle-plastic material: I. Theory." *J. Engrg. Mech.*, ASCE, 114(10), 1672–1680.
- Bažant, Z. P., and Prat, P. C. (1988b). "Microplane model for brittle-plastic material: II. Verification." *J. Engrg. Mech.*, ASCE, 114(10), 1689–1702.
- Carol, I., Bažant, Z. P., and Prat, P. C. (1992). "New explicit microplane model for concrete: Theoretical aspects and numerical implementation." *Int. J. Solids and Struct.*, 29(9), 1173–1191.
- Hasegawa, T., and Bažant, Z. P. (1991). "Nonlocal microplane model with rate effect for concrete." *Struct. Engrg. Rep.*, 91-9/919, Department of Civil Engineering, Northwestern University, Evanston, Ill.
- Hasegawa, T., and Bažant, Z. P. (1993). "Nonlocal microplane concrete model with rate effect and load cycles. II: Application and verification." *J. Mat. In Civ. Engrg.*, ASCE, 5(3), 372–393.

- Ožbolt, J., and Bažant, Z. P. (1991). "Cyclic microplane model for concrete." *Proc. Int. RILEM/ESIS Conf. on fracture processes in brittle disordered materials: concrete, rock, ceramics*, Chapman & Hall, London, England, 639–650.
- Pijaudier-Cabot, G., and Bažant, Z. P. (1987). "Nonlocal damage theory." *J. Engrg. Mech.*, ASCE, 113(10), 1512–1533.
- Taylor, G. I. (1938). "Plastic strain in metals." *J. Inst. Metals*, 62, 307–324.